SIS Mixers using Endfire and Broadside Double Dipole Antennas at 435 and 480 GHz

A. Skalare*,***, M.M.T.M. Dierichs*,**, J. Mees*, H. van de Stadt*, R.A. Panhuyzen*, Th. de Graauw*, T.M. Klapwijk**

* Space Research Organization Netherlands (SRON), Landleven 12, Postbus 800, 9700 AV Groningen, the Netherlands

** Dept. of Applied Physics and Materials Science Centre, University of Groningen, Nijenborgh 4, 9747 AG Groningen, the Netherlands

*** Dept. of Microwave Tech., Chalmers Univ. of Tech., S-412 96 Göteborg, Sweden

Abstract

In the article is presented a double dipole antenna endfire design, which has been fabricated with a two-junction SIS series array. An initial Y-factor measurement gave best performance at 435 GHz, where a receiver noise temperature below 500 K double sideband was achieved. Also presented are measurements with a broadside double dipole array antenna and SIS mixer. An on-chip tuning structure consisting of a short inductive stub, terminated by a lumped niobium oxide capacitor, was used. The best receiver noise temperature achieved was below 200 K DSB at 480 GHz.

1. Introduction

In the latest years, SIS mixers have been generally recognized as the most sensitive devices for heterodyne detection from the mm-wave regime up to frequencies around 500-600 GHz[1]. The most commonly used category is based on waveguide technology, where the detected signal is coupled onto a mixer chip via a horn antenna and a rectangular waveguide. One or two movable short circuits provide microwave matching between the waveguide and the rather capacitive SIS junction. Another category is that of open structure antennas such as bow-ties[2], log-periodic[3], log-spiral[4,5,6,7], ,resonant slot[7], and dipole[8,9,10,11,12,13] antennas. These are all planar structures that are usually fabricated together with the SIS junction itself. The absence of adjustable tuners means that the parasitic capacitance of the junction must be compensated by an on-chip circuit, which in most cases is realized in microstrip technology. Open structure antennas are often mounted directly to a dielectric lens for two different reasons. This is partly to focus down the wide antenna beams, but also to avoid problems associated with substrate modes in the dielectric substrate that supports the antenna and mixer junction.

We will here describe two particular SIS open structure antenna mixers, both using twin dipole arrays in conjunction with dielectric quartz lenses. In the first one the dipole elements are spaced at $\lambda/4$, and are asymmetrically fed by the SIS to create an endfire antenna beam. In the second one the two dipoles are arranged for a broadside beam.

2. An endfire dipole array antenna

2.1 Endfire antenna geometry and design

As is shown in fig. 1, the antenna consisted of two half-wave dipoles that were connected to each other by a co-planar stripline. The overall idea was to choose an appropriate value of the characteristic impedance of the stripline, so that the coupling from each of the two dipole elements to the SIS would be equal in magnitude. With the dipole spacing and the feed point as in Fig. 1, the contributions from the dipole elements add up in phase for one of the endfire directions and out of phase by $\pi/2$ for the other, Fig. 2. The far-field pattern of one of the dipole elements can be approximated by:

$$E_\theta \approx j \cdot \frac{120\pi}{\sqrt{\varepsilon_r}} \cdot \frac{I \cdot e^{-jkr}}{2\pi r} \cdot \frac{\cos\left(\frac{\pi}{2}\cos\theta\right)}{\sin\theta} \qquad \text{Eq. 1}$$

where r is the radius from the dipole to the observation point, θ is the angle between that radius and the axis of the dipole, ε_r is the dielectric constant of the surrounding medium and $k=2\pi/\lambda$. The theoretical diffraction pattern from the two dipoles would then appear as in Fig. 3. The imbalance between the two planes is due to the two extra nulls in the E-plane that are generated by Eq.1 when $\theta \to 0$ and $\theta \to \pi/2$.

The design frequency of the antenna for the SIS mixer chip was 480 GHz, so the length of the dipoles in Fig. 1 was chosen to $\lambda/2$=160 μm, where the dielectric constant of the surrounding fused silica medium was taken into account (ε_r=3.8). The width of the dipole elements was 24 μm, and the width and spacing of the coplanar stripline between them were 8 and 4 μm, respectively. The DC/IF connection to the SIS was made via the wires to the right in Fig. 1. A band stop filter consisting of 7 $\lambda/4$ sections was used to prevent RF leakage to the line. The width and spacing of the high impedance sections were 4 and 20 μm, respectively, and of the low impedance sections 20 and 4 μm. Each SIS junction was connected to a 75 μm long open ended tuning stub of width 4 μm. 250 nm of SiO_2 was used as dielectric for the stubs. The two Nb-Al/AlOx-Nb SIS junctions had an area of ≈1.5 μm^2 and a total normal resistance of 29 Ω.

The mixer chip was glued to the back plane of a fused silica lens with cyanoacrylat glue, Fig. 4. The chip was supported by two other glued-in fused silica pieces, which also ensured that the dipole antenna would be completely surrounded by the same dielectric material. The lens had a diameter of 11 mm, and had the unique ellipsoidal shape that would focus a plane wave into a point, according to geometrical optics. The edge of the mixer chip had previously been sawed so that this focal point would fall halfway between the dipoles.

2.2 Endfire antenna measurements

The fused silica lens with the endfire dipole SIS chip was placed in a fixture inside an SIS receiver cryostat. The first measurements were made with a *Fourier Transform Spectrometer* (FTS), and after that a Y-factor measurement was carried out. The

fixture holding the lens and the Y-factor measurements will be described in the later section about the broadside antenna chip measurements.

The spectrogram from the FTS measurement showed two response peaks, Fig. 5. The first was a sharp peak at 320 GHz, and the second one a slightly broader shape from 450 to 470 GHz. This latter response was the result of the tuning stubs connected to the SIS junctions, and fell within the 402-496 GHz range of the carcinotron source in our Y-factor measurement set-up. It is not known what caused the 320 GHz peak. The SIS DC bias voltage was 4.92 mV (2.46 mV per junction).

The noise measurements showed a best Y-factor response of 1.4 dB at 435 GHz, with the local oscillator power coupled in via a 60 μm Mylar™ beamsplitter at 45° angle in front of the dewar window. With the hot and cold loads at 290 and 77 K, respectively, this corresponds to a double sideband noise temperature of 483 K. As the transmission of the beamsplitter was rather low, only ≈ 62%, we feel the results could be improved significantly by using a thinner one. The same measurement set-up was used as in the broadside dipole measurements that are described below. Fig. 6 shows the noise temperature as a function of frequency, measured at an intermediate frequency of 4.3 GHz. Fig. 7 shows an unpumped and a pumped IV curve, together with the mixer output.

3. Broadside dipole array antenna

3.1 Broadside antenna geometry and design

The design and some properties of the broadside double dipole antenna have been described in the references[12,14]. As is shown in Fig. 8, the antenna consists of two planar half-wave dipoles, that are separated by slightly less than half a wavelength. The dipoles are connected by a co-planar stripline, with the feed point at the center. The DC and intermediate frequency connections are via the co-planar stripline to the right in Fig. 8. A 7-section lambda quarter bandstop filter prevents leakage of signal and local oscillator power along the line. On the mixer chip a single 1.5 μm^2 Nb-Al/AlOx-Nb SIS junction was fabricated at the feed point of the antenna. The junction capacitance was tuned by a short microstrip section, which was shunted to ground at the end by a 25 μm^2 large lumped capacitor. The microstrip had a width of 1.6 μm, and used a 250 nm thick SiO_2 layer as dielectric. Several lengths were patterned on different chips, but the measurements we report here were all made with a device where the stub length was ≈ 6.2 μm. The shunt capacitor was formed by defining a large extra SIS junction, the top electrode and oxide barrier of which was later etched away, thereby exposing the niobium of the base electrode. An extra anodization step was carried out to create approximately 50 nm of Nb_2O_5, which was used as dielectric. The purpose of the capacitor was to create an approximate short circuit at the signal and local oscillator (LO) frequencies, without shorting out the DC bias and the IF output from the mixer. At the signal and LO frequencies, this places the microstrip "inductance" in shunt with the junction capacitance. This arrangement provides a larger bandwidth than a simple open ended stub, and requires less surface space on the antenna.

The antenna chip was glued with cyanoacrylat to the back plane of a fused silica hyperhemispheric lens of 11 mm diameter, Fig. 9. An 80 μm thick fused silica chip with a deposited chromium/gold reflector on one side was glued on to the antenna chip. The thickness of the lens had been chosen so that the focus would fall on the reflector, where the phase center of this antenna should be.

The lens was held by the fixture in Fig. 10. It was cooled via the copper front and back plates and via the copper braid. An extra cooling strap of copper foil was glued directly to the reflector chip with silver paint. The flexible copper/Kapton™/copper strip line that was used for the DC and IF connections to the mixer chip is described in one of the references[14]. A superconducting magnet was placed to the side of the fixture for suppression of the Josephson effect. The same mixer fixture and magnet were also used in the measurements with the endfire antenna, but with the magnet placed directly behind the fixture instead of to the side. The objective with that was to orient the magnetic field into the plane of the SIS junctions.

3.2 Broadside antenna Y-factor measurements at 480 GHz

Y-factor measurements were carried out between 420 and 496 GHz with the set-up shown in Fig. 11. The mixer fixture and magnet were attached to the cold plate of an Infrared Labs. HD(3)-8 cryostat. The signal and local oscillator were coupled in through a TPX window, and focused onto the fixture with a polyethylene lens. A 200 μm thick fused silica sheet was used to reduce the heat flow into the cryostat. The intermediate frequency output from the mixer was connected to a Berkshire Tech. HEMT amplifier, with a best performance according to the manufacturer of 3.7 K at 4.4 GHz. This frequency was also our choice for the broadside antenna measurements.

In the first measurement, a rather thick Mylar beamsplitter was used (60 μm). This resulted in the noise temperatures shown in Fig. 12, with a best point just below 400 K DSB at 480 GHz. A second measurement was made with a 15 μm Mylar beamsplitter, which gave a best hot/cold response of 2.5 dB at 470 and 480 GHz. With the hot and cold loads at 290 and 77 K, respectively, this gives a best receiver noise temperature of just below 200 K DSB. Fig. 13 shows the unpumped IV curve together with a pumped curve and the hot and cold load responses at 480 GHz.

4. Summary

An SIS mixer using an endfire double dipole antenna was presented. A simplified theoretical analysis shows a that the main lobe is rather wide, and not of the same width in the E- and H-planes. The SIS mixer chip was mounted on the back side of an ellipsoidal fused silica lens. A measurement of the broadband coupling to the SIS was made with a Fourier transform spectrometer, which showed that the on-chip superconducting microstrip stubs tuned out the junction capacitance at around 460 GHz. Y-factor measurements showed a response slightly lower in frequency. The best noise temperature point was just below 500 K DSB at 435 GHz, measured with a 60 μm beamsplitter. This value should be improved if a thinner beamsplitter is used.

The 480 GHz receiver used a broadside double dipole antenna with a single SIS junction. The junction capacitance was tuned out with a short inductive stub that was terminated in a lumped capacitor. The mixer chip was mounted on the back side of a hyperhemispherical fused silica lens, and a Y-factor measurement was made. The best performance was at 470 and 4809 GHz, where the Y-factor was 2.5 dB. This gives a noise temperature of less than 200 K DSB. The bandwidth, measured at the 300 K DSB level, was more than 30 GHz.

Acknowledgements

We would like to acknowledge Harry Schaeffer for much mechanical design work (including the superconducting magnets) and Johan Wezelman for help with many measurements. Both are with the Space Research Organization, the Netherlands. We would also like to thank Niklas Rorsman of Chalmers University, Sweden, for manufacturing our E-beam masks. We also thank Dr. Errico Armandillo of the European Space Agency at ESA/ESTEC in Noordwijk, the Netherlands, for his financial support of this project through contract 7898/88/Pb/(Sc).

References

1 R. Blundell, Cheuk-Yu E. Tong, "Submillimeter Receivers for Radio Astronomy", Proceedings of the IEEE, Vol.80, No.11, Nov.1992.

2 X.Li, P.L. Richards, F.L. Lloyd, "SIS Quasiparticle Mixers with Bow-Tie Antennas", Int. J. of Infrared and Millimeter Waves, Vol.9, pp.101-103, 1988.

3 R.H. DuHamel, D.E. Isbell, "Broadband Logarithmically Periodic Antenna Structures", 1957 IRE National Convention Record, pt.1, pp.119-128.

4 J.D. Dyson, "The Equiangular Spiral Antenna", IRE Trans. Antennas Propag., Vol. AP-7, pp. 181-187, April 1959.

5 T.H. Büttgenbach, R.E. Miller, M.G. Wengler, D.M. Watson, T.G. Phillips, "A Broad-Band Low-Noise SIS Receiver for Submillimeter Astronomy", IEEE Trans. Microwave Theory Tech., Vol. MTT-36, pp. 1720-1726, Dec. 1985.

6 B. Yu. Belitsky, I. L. Serpuchenko, M. A. Tarasov, A. N. Vystavkin, "MM Waves Detection using Integrated Structure with SIS Junction, Stripline Transformer and Spiral Antenna", Extended Abstracts of ISEC-89, Tokyo, 1989, pp.179-182.

7 J. Zmuidzinas, H.G. LeDuc, "Quasi-Optical Slot Antenna SIS Mixers", IEEE Trans. Microwave Theory Tech., Vol.40, No.9, September 1992.

8 P. T. Parrish, T. C. L. G. Sollner, R. H. Mathews, H. R. Fetterman, C. D. Parker, P. E. Tannenwald, A. G. Cardiasmenos, "Printed Dipole-Schottky Diode Millimeter Wave Antenna Array", SPIE Millimeter Wave Technology, Vol. 337, 1982, pp.49-52

9 W. Chew, H. R. Fetterman, "Printed Circuit Antennas with Integrated FET Detectors for mm-Wave Quasi-Optics", IEEE Trans. Microwave Theory Tech., Vol. MTT-37, No. 3, 1989.

10 J. A. Taylor, T. C. L. G. Sollner, D. D. Parker, J. A. Calviello, "Planar Dipole-fed Mixer Arrays for Imaging at Millimeter and Sub-Millimeter Wavelenghts", Proc. of the 1985 Int. Conf. on IR and mm-Waves, 1985, pp.197-188.

11 H. Rothermel, D. Billon-Pierron, K. H. Gundlach, "An Open Structure SIS Mixer for 350 GHz", Presented at the 16th Int. Symp. of Infrared & Millimeter Waves, Lausanne, Switzerland, Aug. 1991.

12 A. Skalare, Th. de Graauw, H. van de Stadt, "A Planar Dipole Antenna with an Elliptical Lens", Microwave & Optical Tech. Letters, Vol.4, No.1, January 1991.

13 K. Uehara, K. Miyashita, K.-I. Natsume, K. Hatakeyama, K. Mizuno, "Lens-Coupled Imaging Arrays for the Millimeter- and Submillimeter-Wave Regions", IEEE Trans. Microwave Theory Tech., Vol. MTT-40, No. 5, 1992.

14 A. Skalare, H. van de Stadt, Th. de Graauw, R. A. Panhuyzen, M. M. T. M. Dierichs, "Double Dipole Antennas at 100 and 400 GHz", Proc. Third Int. Symp. on Space Terahertz Tech., Ann Arbor, Michigan, U.S.A., March 24-26, 1992.

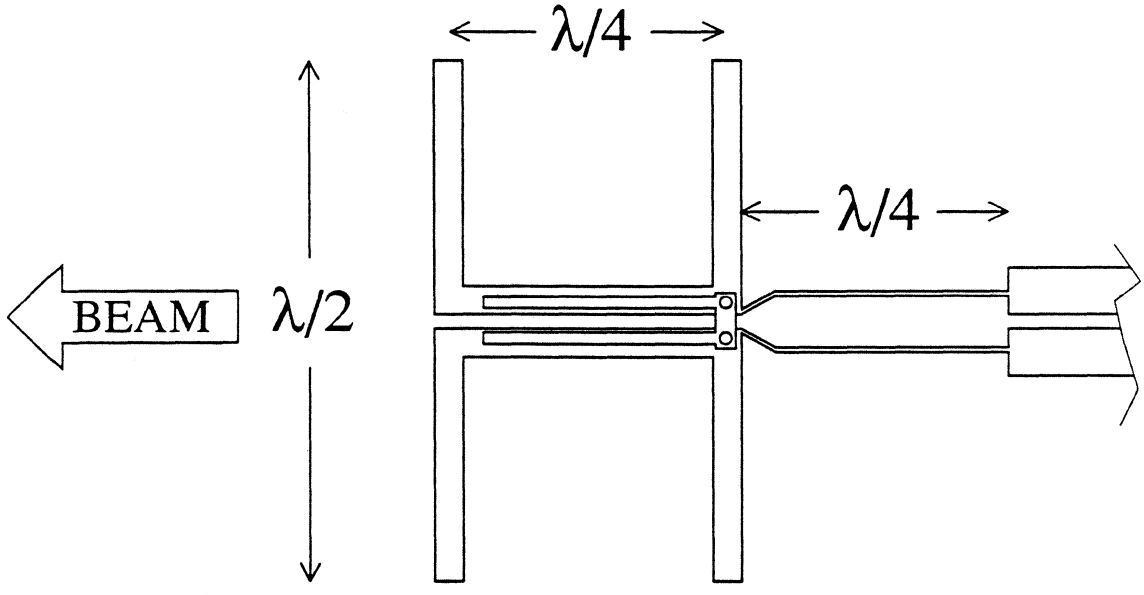

Fig. 1: The endfire double dipole antenna.

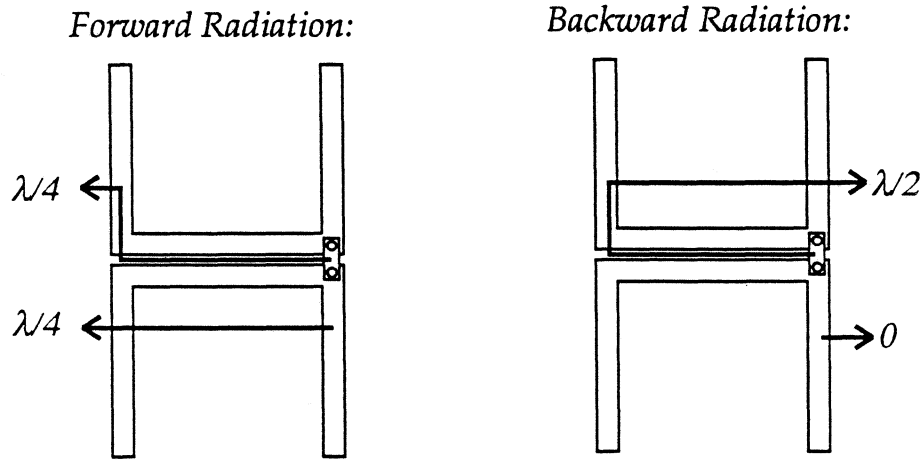

Fig. 2: The contributions from the two dipole elements add up in phase in one endfire direction, and cancel each other out in the other.

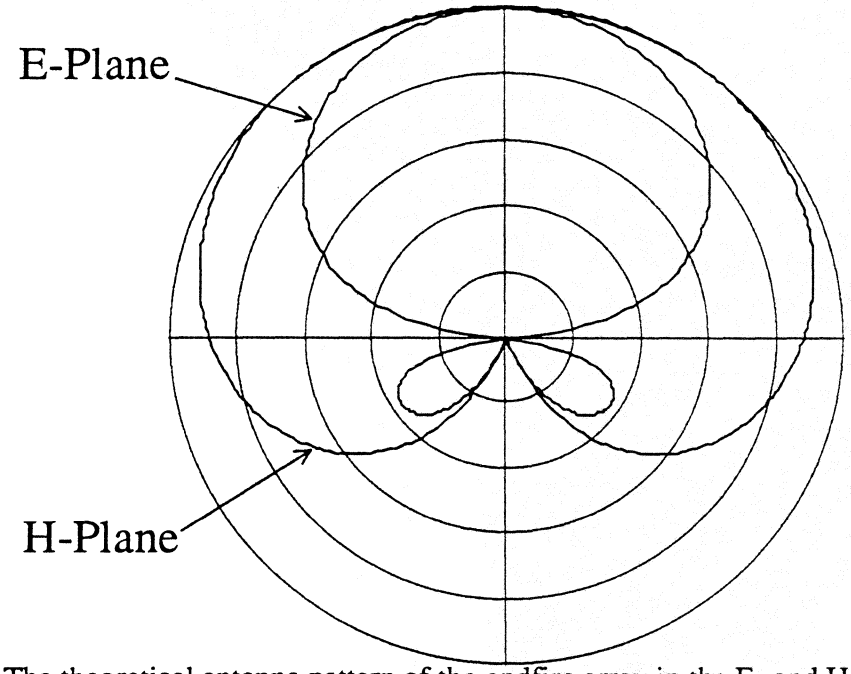

Fig. 3: The theoretical antenna pattern of the endfire array in the E- and H-planes. The radial scale is 5 dB per division.

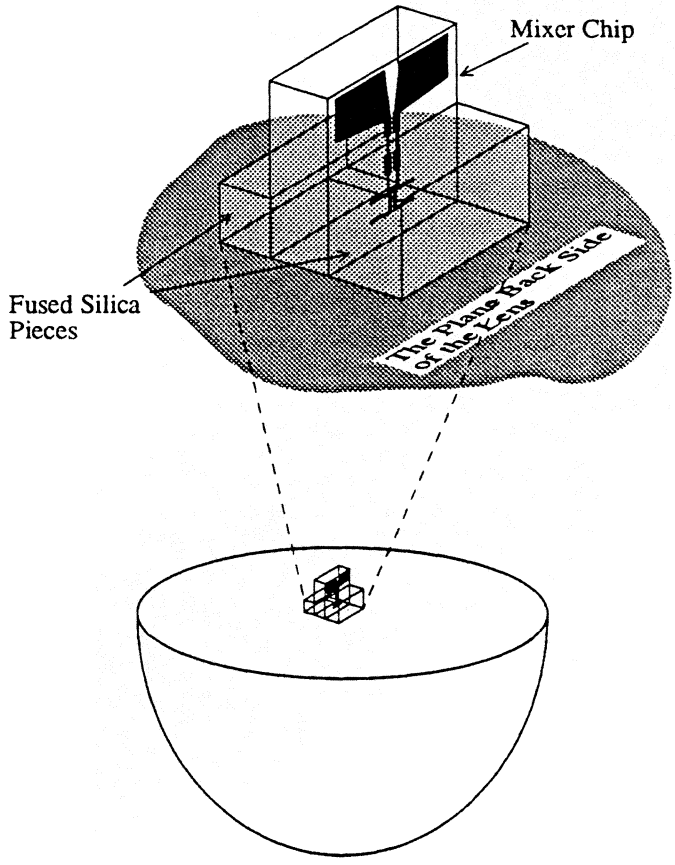

Fig. 4: How the endfire dipole chip is glued to the back plane of the lens. The figure is not true to scale.

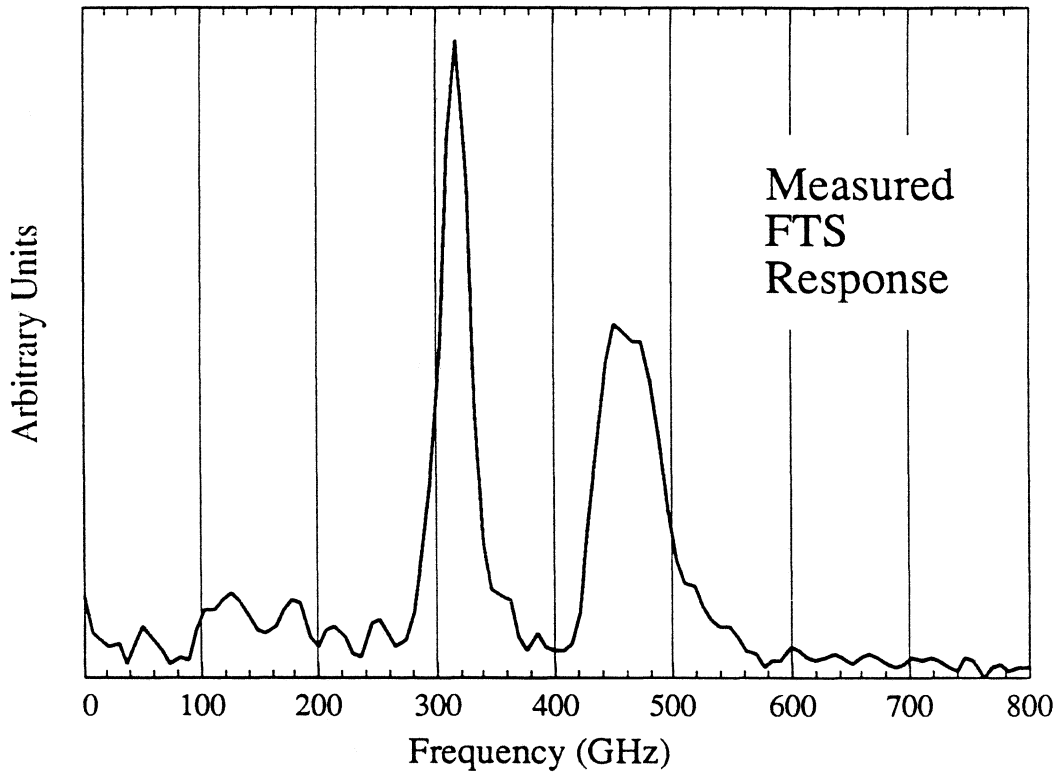

Fig. 5: Response of the SIS endfire dipole antenna chip, as measured with a Fourier transform spectrometer.

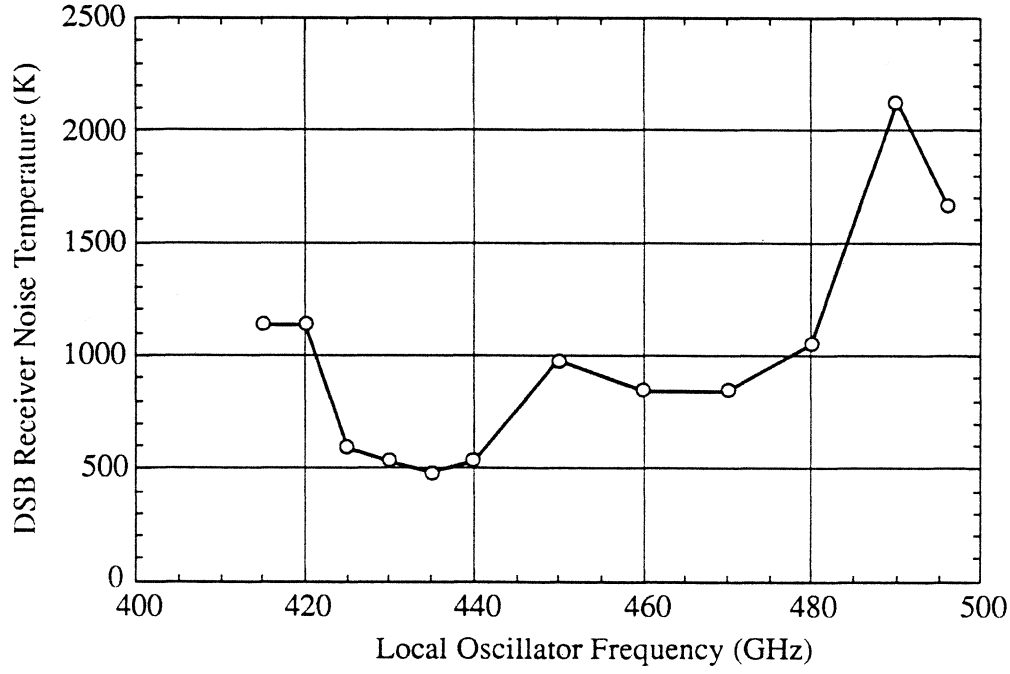

Fig. 6: The double sideband noise temperatures of the SIS endfire dipole antenna receiver.

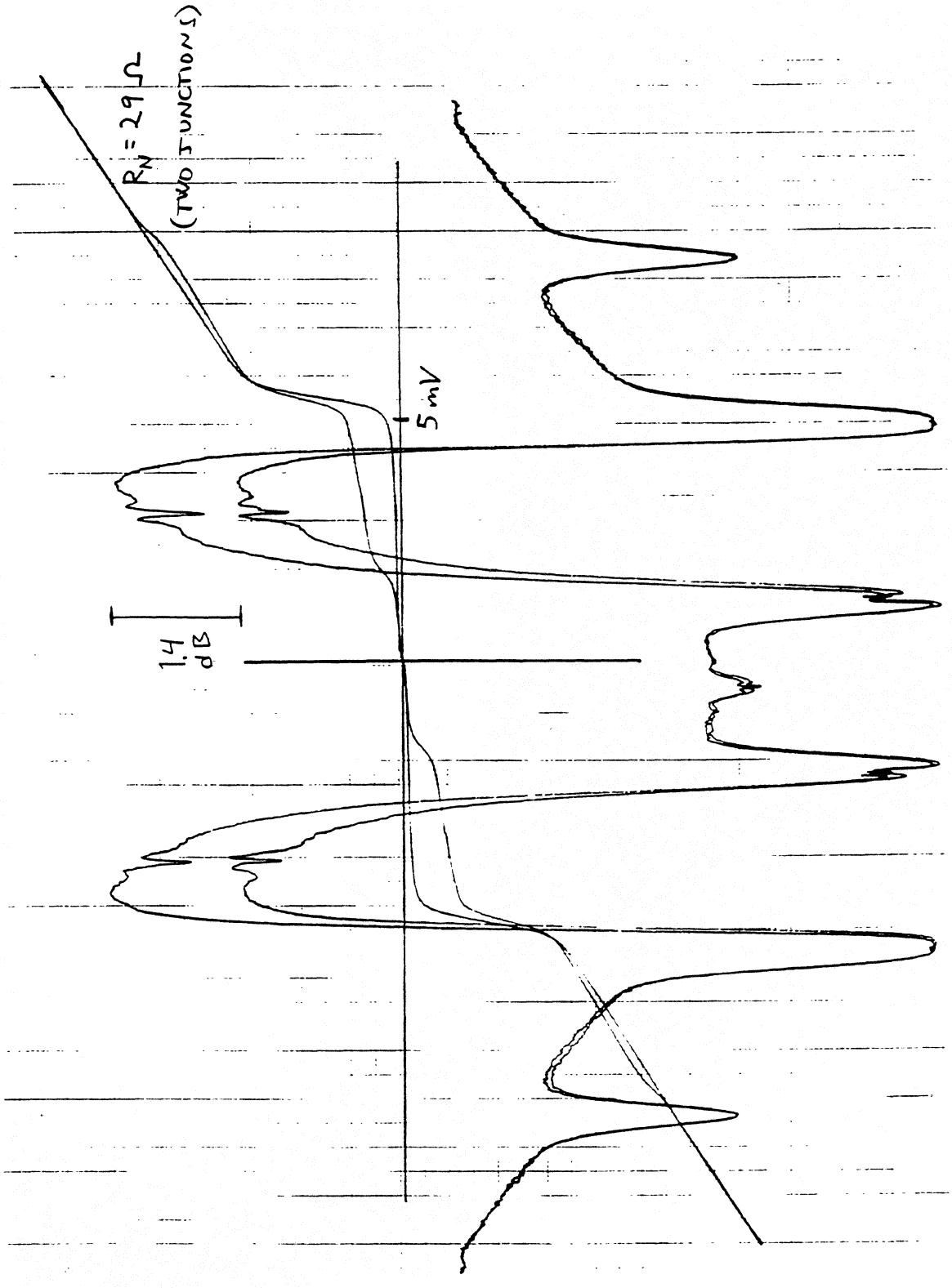

Fig. 7: Unpumped and pumped DC IV curves of the endfire antenna SIS junctions. The pump frequency was 435 GHz. Also shown is the intermediate frequency output at 4.3 GHz.

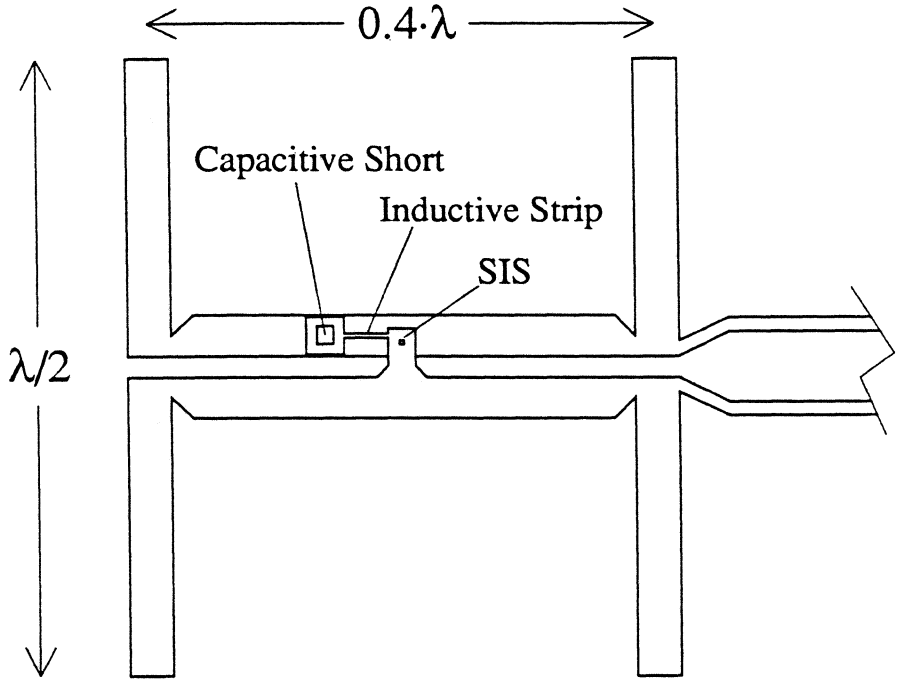

Fig. 8: The broadside dipole array antenna. "λ" is the wavelength in fused silica at 430 GHz (358 μm). All dimensions except the length of the inductive strip are shown true to scale.

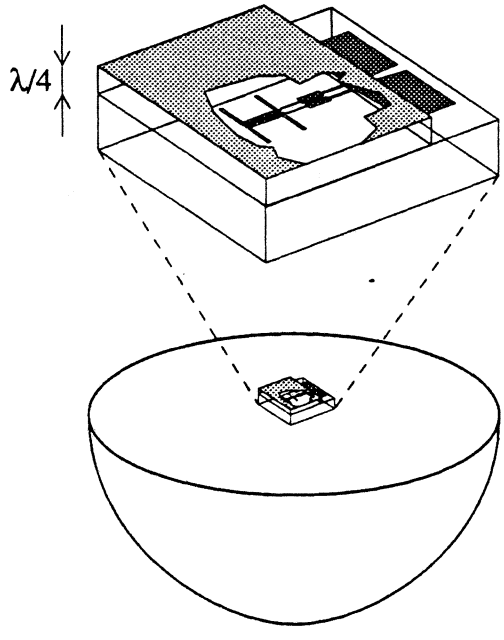

Fig. 9: A schematic view of how the broadside antenna chip is mounted to the lens. Part of the Cr/Au reflector has been removed to expose the antenna.

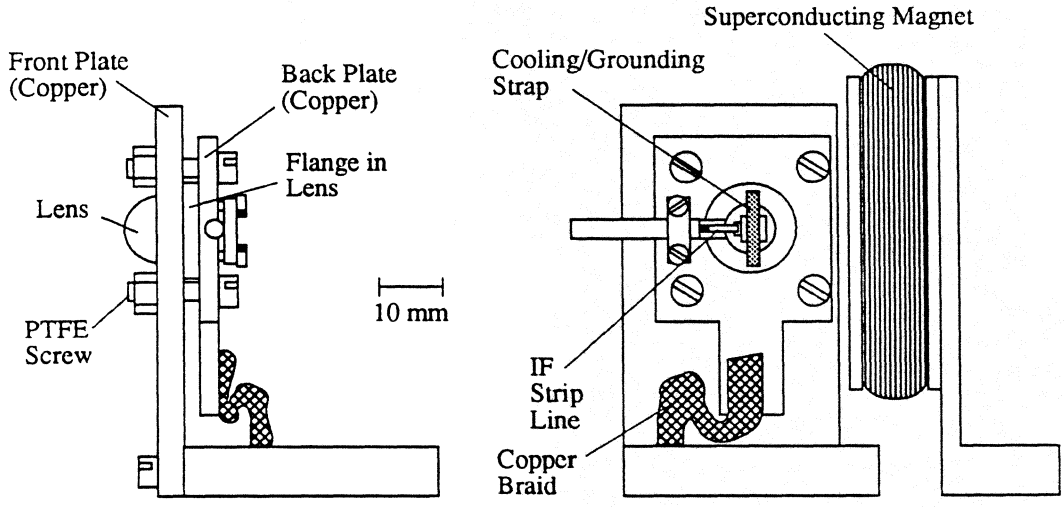

Fig. 10: The mixer fixture used in the measurements with the broadside antenna SIS chip.

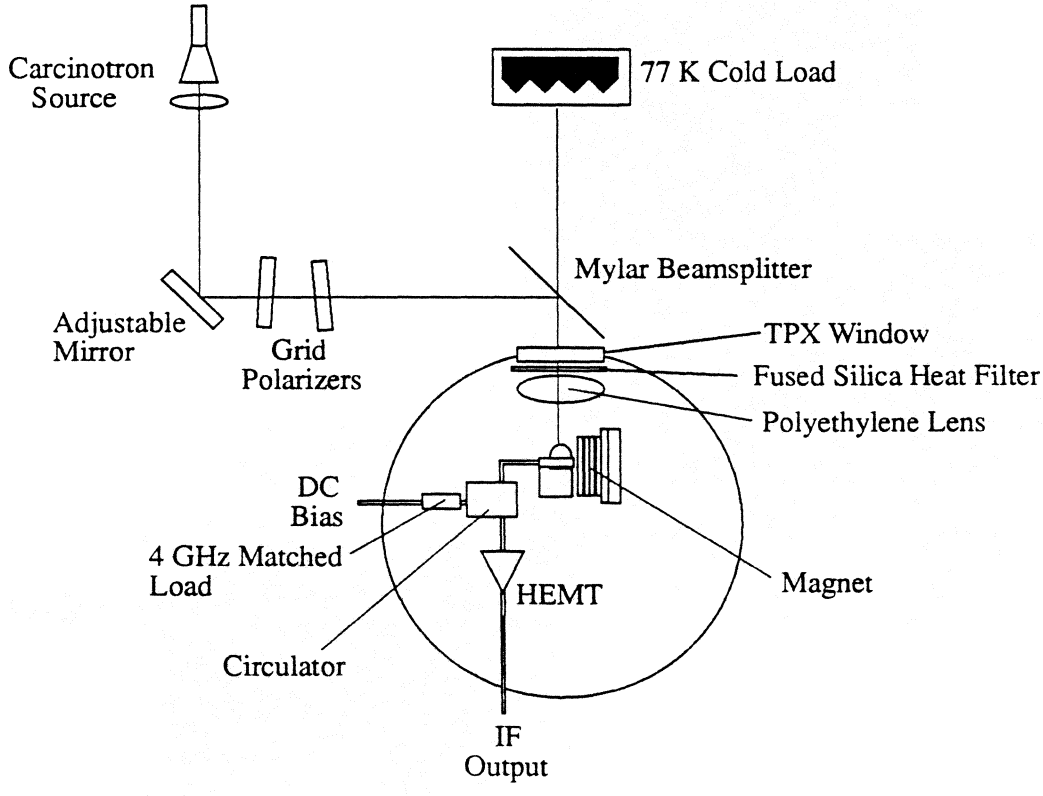

Fig. 11: The 420-496 GHz Y-factor set-up for the measurement with the broadside antenna chip.

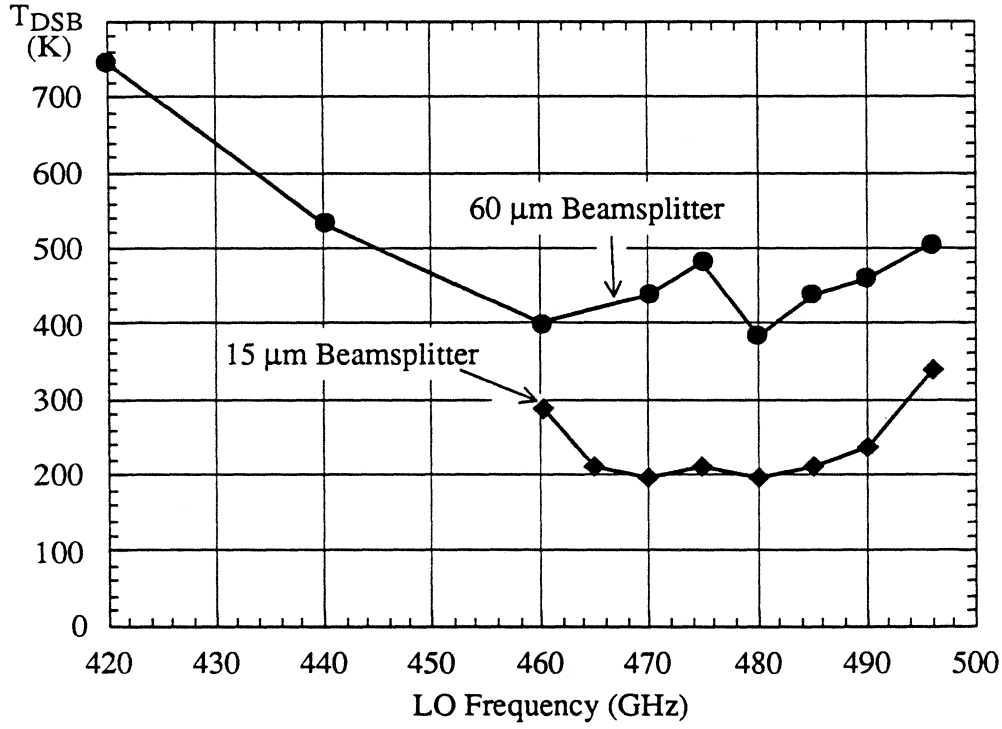

Fig. 12: Noise temperature results from the Y-factor measurements with the broadside antenna chip.

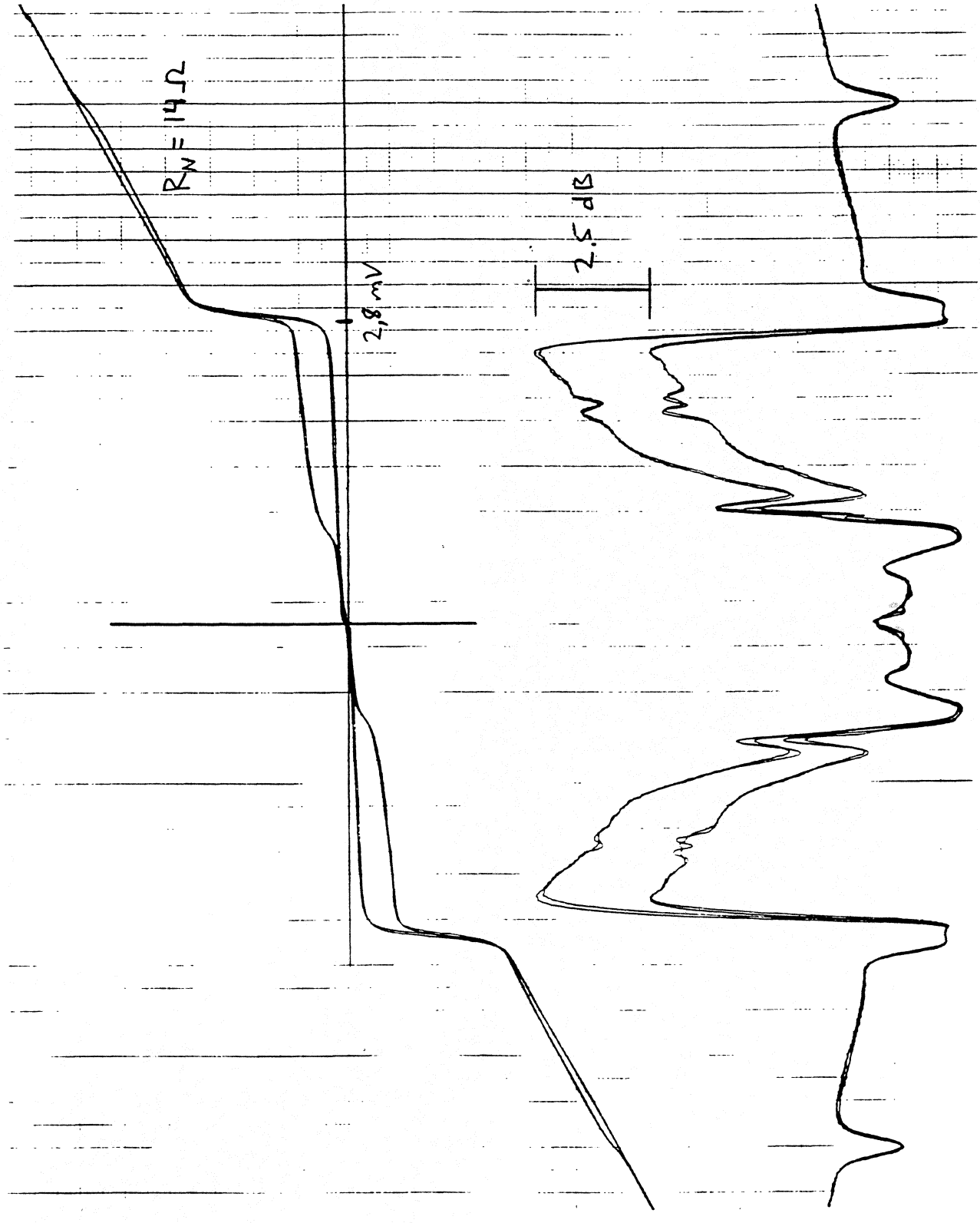

Fig. 13: Unpumped and pumped (480 GHz) DC IV curves of the broadside SIS junctions. Also shown is the intermediate frequency output at 4.3 GHz.